

# First-principles prediction of crystal structures at high temperatures using the quasiharmonic approximation

Pierre Carrier and Renata Wentzcovitch

*Minnesota Supercomputing Institute and Department of Chemical Engineering and Materials Science, University of Minnesota, Minneapolis, Minnesota 55455, USA*

Jun Tsuchiya

*Geodynamics Research Center, Ehime University, Matsuyama, Japan*

(Received 27 April 2007; revised manuscript received 19 July 2007; published 23 August 2007)

We show here how first-principles quasiharmonic approximation (QHA) calculations in its simplest statically constrained form can be used to predict crystal structures at high temperatures. This approximation has been extensively used to investigate thermodynamic properties of Earth forming minerals and has offered excellent results for the major mantle phases at relevant conditions. We carefully compare QHA predictions of crystal structures using the local density approximation with crystallographic data in  $\text{MgSiO}_3$  perovskite at high pressures and temperatures. Small but systematic deviations in the lattice parameters (at most 0.3%) appear at high temperatures ( $T > 2000$  K) and are associated with the development of deviatoric thermal stresses. An iterative scheme is proposed to eliminate these spurious thermal stresses and further improve the quality of the predictions of this popular and successful thermodynamics method.

DOI: [10.1103/PhysRevB.76.064116](https://doi.org/10.1103/PhysRevB.76.064116)

PACS number(s): 62.20.Dc, 65.40.-b, 91.35.-x, 91.60.Gf

## I. INTRODUCTION

The quasiharmonic approximation<sup>1</sup> (QHA) is a simple and powerful method for evaluating free energies using density functional theory.<sup>2</sup> As opposed to molecular dynamics, its only available alternative so far, the QHA remains inexpensive computationally and valid below the Debye temperature. Here, we describe its simplest and most used form, the statically constrained QHA, indicate its conditions of validity, test its predictions for crystal structures against experimental data, and show that the quality of these predictions can be further improved by the relaxation of deviatoric thermal stresses. An ideal QHA calculation should, therefore, involve a self-consistent cycle that minimizes deviatoric thermal stresses to a predefined level, and we propose a systematic scheme to achieve this. Systematic approaches are important especially when investigating materials with a large number of structural parameters. Crystallographic measurements at combined high pressures and temperatures are also very challenging, and there are few studies to date<sup>3</sup> that combine both high pressures and temperatures. In addition, most of these measurements register only lattice parameters, not internal ones.

As an example, we chose  $\text{MgSiO}_3$  perovskite (pv), the most abundant mineral in the Earth's mantle. It has a non-trivial crystal structure with 20 atoms per unit cell and ten structural degrees of freedom, and is one of the most studied materials at high pressures and temperatures.<sup>4-9</sup> Current crystallographic data on  $\text{MgSiO}_3$  pv vary up to 60 GPa and 2600 K, a condition pertaining to the Earth's lower mantle. We analyze and explain why predictions of the QHA compare well with experiments and, most importantly, why they should be reliable at Earth's lower mantle conditions.

## II. STATICALLY CONSTRAINED QUASIHARMONIC APPROXIMATION

The free energy according to the statically constrained QHA is given by

$$F(V, T) = \left[ U(V) + \sum_{\mathbf{qj}} \frac{\hbar \omega_{\mathbf{qj}}(V)}{2} \right] + k_B T \sum_{\mathbf{qj}} \ln(1 - e^{\hbar \omega_{\mathbf{qj}}(V)/k_B T}), \quad (1)$$

where  $U(V)$  is the static energy versus volume obtained after a full structural relaxation under isotropic pressure.  $\omega(V)$  is the phonon spectrum at these fully relaxed structures. The second term is the zero-point motion energy  $F_{ZP}$ , and the sum of the two terms in brackets is the energy at  $T=0$  K. The last term in Eq. (1) is the thermal excitation energy  $F_{th}$ . Boltzmann's and Planck's constants are, respectively,  $k_B$  and  $\hbar$ . The entropy  $S$  and pressure  $P$  are then obtained from  $F$  using standard thermodynamic relations,<sup>1</sup>

$$S = - \left. \frac{\partial F}{\partial T} \right|_V \quad \text{and} \quad P = - \left. \frac{\partial F}{\partial V} \right|_T. \quad (2)$$

The known quantities  $U$ ,  $T$ ,  $V$ ,  $S$ , and  $P$  directly give the Gibbs free energy

$$G = U - TS + PV. \quad (3)$$

The isothermal elastic moduli can then be evaluated from the second derivative of  $G$  with respect to the strains  $\epsilon_i$  and  $\epsilon_j$  (in Voigt's notation),

$$c_{ij}^T(P, T) = \left. \frac{\partial^2 G}{\partial \epsilon_i \partial \epsilon_j} \right|_{P, T}. \quad (4)$$

At this point, it is fundamental to note that the crystal structure and phonon frequencies depend on *volume* alone.

This is because all structural parameters under pressure have been determined by static calculations and are given at  $P_{stat}(V)$  only. Note that at a certain  $V$ ,  $P_{stat}$  indeed depends on the exchange correlation functional used, but since the structure/volume relation depends only mildly on this functional, structural predictions at high  $P$ - $T$ 's through volumetric effects carry only a very mild dependence on the functional. Then, at  $T=T'$ , the pressure  $P'(V, T')$ , evaluated using expressions (1) and (2), contains contributions from zero-point and thermal energies, i.e.,  $P' = P_{stat} + P_{ZP} + P_{th}$ , where

$$P_{ZP} = \left. \frac{-\partial F_{ZP}(V, T)}{\partial V} \right|_{T'} \quad \text{and} \quad P_{th} = \left. \frac{-\partial F_{th}(V, T)}{\partial V} \right|_{T'}. \quad (5)$$

No further structural relaxation is performed at  $T'$ . The function  $V(P', T')$  is then obtained after inverting  $P'(V, T')$ . Therefore, in this statically constrained QHA calculation, if  $V(P', T') = V(P_{stat})$ , then structural parameters and phonon frequencies at  $(P', T')$  and at  $P_{stat}(V)$  are the same.

This fundamental consequence of the *statically constrained* QHA can be tested against high  $P$ - $T$  experimental data of  $\text{MgSiO}_3$  pv. This is a direct test of the accuracy of this approximation. If the test is favorable, this procedure can be used to predict structures at high  $P$ - $T$ 's.  $\text{MgSiO}_3$  pv has an orthorhombic structure with the symmetry group  $Pbnm$ . The unit cell contains 20 atoms. Simultaneously ten structural parameters must be relaxed: the three lattice parameters  $\mathbf{a}$ ,  $\mathbf{b}$ , and  $\mathbf{c}$  plus the seven internal parameters. Optimization of  $\text{MgSiO}_3$  pv is performed using the variable cell shape molecular dynamics method,<sup>10</sup> using the quantum ESPRESSO package.<sup>11</sup> Phonon dispersions were computed using linear response theory.<sup>12</sup> They have been reported<sup>13</sup> and used for elasticity calculations<sup>14</sup> in earlier publication.

Before making comparisons with experiments, one must be careful to limit this comparison to the  $P$ - $T$  domain where quasiharmonic predictions are expected to be reliable. This  $P$ - $T$  domain can be defined by *a posteriori* inspection of the thermal expansivity,<sup>14</sup>

$$\alpha = - \left. \frac{1}{V} \frac{\partial V}{\partial T} \right|_{P'}, \quad (6)$$

resulting from statically constrained calculations. Experiments show that at high temperatures,  $\alpha$  should increase linearly with  $T$ .<sup>15</sup> However, quasiharmonic calculations display a superlinear behavior. Figure 1 shows the calculated thermal expansivity as a function of temperature for various pressures applied to  $\text{MgSiO}_3$  pv. The inflection points of  $\alpha$ , as defined by  $\partial^2 \alpha / \partial T^2|_P = 0$ , correspond to the locus where  $\alpha$  starts to vary superlinearly with increasing temperature. Therefore, the inflection curve of  $\alpha$  constitutes a realistic criterion for separating the domain of validity of the QHA from the invalid regions. This boundary is labeled “QHA boundary” in Fig. 1. In all figures, solid and dashed lines are used for predictions made within and outside the regime of validity of the QHA, respectively. We remark that the higher the pressure, the larger the temperature domain of validity of

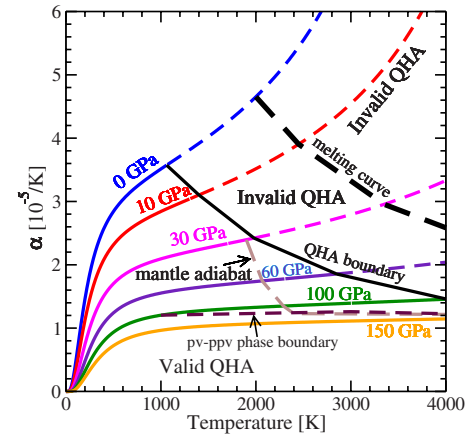


FIG. 1. (Color online) Thermal expansivity as a function of temperature for various pressures. The black line, labeled “QHA boundary,” is defined by the position of the inflection points of  $\alpha(P, T)$ , as described in the text. The melting curve (Ref. 16), the location of the mantle adiabat (Ref. 19), and the postperovskite phase boundary (Ref. 14) are also shown.

the QHA, indicating that anharmonicities decrease with pressure in the absence of phonon softening. The location of the experimental melting curve of Zerr and Boehler<sup>16</sup> is also shown. At melting, anharmonic interactions are no longer negligible.<sup>17,18</sup> As can be seen, the valid QHA domain is clearly well below the melting curve. The QHA also remains valid along the whole mantle geotherm,<sup>19</sup> except maybe at conditions at the top of the lower mantle, i.e., 23.5 GPa where  $\text{MgSiO}_3$  pv becomes the stable structure. We finally

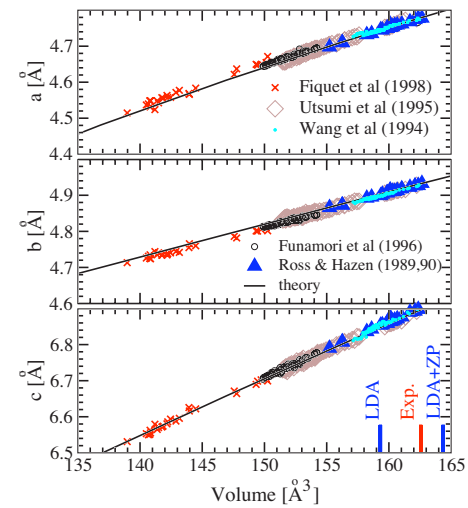


FIG. 2. (Color online) Comparison between lattice parameters predicted by the QHA and experimental data as a function of volume. The LDA and LDA plus zero-point motion equilibrium volumes are also compared to the experimental equilibrium volume at 0 GPa. Experimental data are from Refs. 4–9. Temperatures vary from 295 to 1024 K for Wang *et al.* (Ref. 9), from 293 to 2668 K for Fiquet *et al.* (Ref. 4), from 298 to 1173 K for Utsumi *et al.* (Ref. 8), from 293 to 2000 K for Funamori *et al.* (Ref. 5), and from 77 to 400 K for Ross and Hazen (Ref. 6 and 7). Solid lines are from theory.

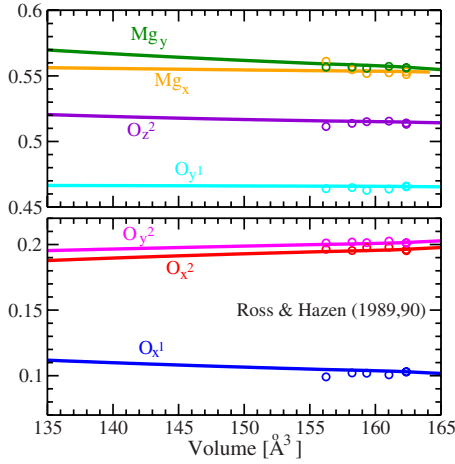


FIG. 3. (Color online) Comparison between internal parameters predicted by the QHA (solid lines) and experiments (data points) as a function of volume. Experimental data are from Refs. 6 and 7.

notice that the postperovskite (ppv) transition phase boundary<sup>20</sup> falls within the domain of validity of the QHA for pv and ppv phases.

Figure 2 shows the variation of lattice parameters **a**, **b**, and **c** as functions of volume obtained by several high  $P$ - $T$  experiments (data points) as compared with the static local density approximation (LDA) prediction (full line). Figure 3 shows the same variation now for the internal parameters, as compared to available experimental data points. Experiments were performed under various  $P$ - $T$ 's, for temperatures varying from 70 (Refs. 6 and 7) to above  $\sim 2600$  K [e.g., in Funamori *et al.*,  $T$ 's vary from 293 to 2000 K (Ref. 5); in Fiquet *et al.*,  $T$ 's vary from 293 to 2668 K (Ref. 4)] and pressures varying between 0 and 60 GPa. Clearly, from Fig. 2, *all* experimental lattice parameters obtained at various  $P$ - $T$ 's lie on or very close to the theoretical lines. Additional experimental data should test (likely confirm) the trend for the internal parameters shown in Fig. 3. These results indicate that, indeed as predicted, the statically constrained QHA is a good approximation in the  $P$ - $T$  range of these experiments. We also indicate in Fig. 2 the LDA equilibrium volume at 0 GPa, including (not including) zero-point (ZP) motion energy, LDA+ZP, and compare both with the experimental value.<sup>6,13</sup> The inclusion of ZP motion increases the equilibrium volume at zero pressure. It becomes larger than, but in better agreement with, the experimental zero pressure volume. A similar trend has been found for all other mantle silicates and oxides investigated by this method so far.

A closer examination of Fig. 2 at small volumes (i.e., higher pressures) shows that although all experimental data lie close to the predicted theoretical straight lines, there exist still some small but systematic deviations. Some of these data points include very high temperature data. For instance, both data of Fiquet *et al.* and of Funamori *et al.* for the lattice parameter **a** are slightly larger than the QHA prediction. The discrepancy is of the order of 0.3% or 0.01 Å. The opposite is observed for the lattice parameter **b**. The discrepancy in this case is of the order of  $-0.1\%$  or  $-0.005$  Å. No clear

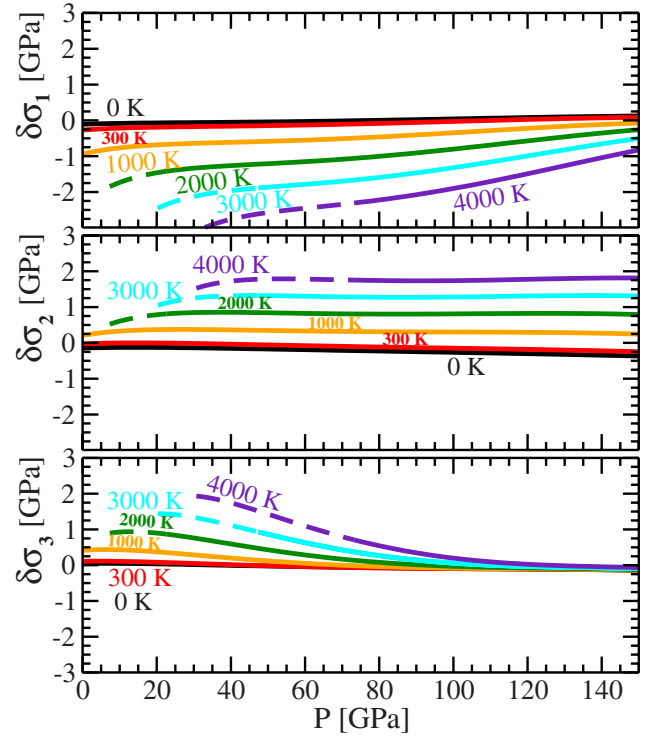


FIG. 4. (Color online) Deviatoric stresses [see Eq. (7)] along **a**, **b**, and **c** axes.

discrepancies are noticeable in the lattice parameter **c**. Although minor, these discrepancies remain systematic and could originate either in the LDA or in the QHA. In the following, we address this problem.

### III. DEVIATORIC THERMAL STRESS RELAXATION

In the statically constrained QHA, energies are computed according to Eq. (1) and pressures according to Eq. (2). This procedure implicitly assumes that pressure remains isotropic *at all temperatures*, but this is only true for static calculations. The zero-point motion and the thermal pressure contributions to  $P'$  are not necessarily isotropic. This effect is explicitly quantified by the deviatoric stresses defined as the difference between the nominal pressure and the diagonal stress components,

$$\delta\sigma_i = P' - \left[ -\frac{1}{V} \frac{\partial G(P, T)}{\partial \epsilon_i} \right]_{P', T'}. \quad (7)$$

Figure 4 shows these deviatoric stresses versus  $P$  along the crystalline directions [100], [010], and [001] at various  $T$ 's. With increasing  $T$ ,  $\delta\sigma_1$  becomes more negative. This means that the statically constrained system becomes over-compressed along [100] at high  $T$ 's. The opposite appears along [010], and minor changes affect the [001] direction. This result is consistent with Fig. 2, where the experimental data lie above the static QHA for **a**, below for **b**, and essentially on top for **c**.

These deviatoric stresses can be relaxed to first order if one knows the compliance tensor  $\kappa_{ij}(P', T') = c_{ij}^{-1}(P', T')$ ,

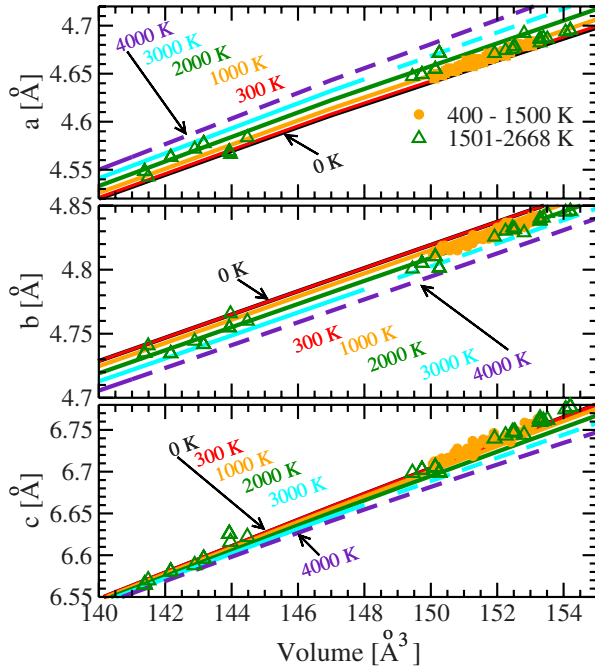


FIG. 5. (Color online) Corrected lattice parameters  $[a - \epsilon_1 a]$ ,  $[b - \epsilon_2 b]$ , and  $[c - \epsilon_3 c]$  where  $\epsilon_i$ 's are solutions of Eq. (8), compared with the data of Funamori *et al.* (Ref. 5) data between 400 and 1500 K (orange dots) and Fiquet *et al.*<sup>4</sup> data above 1500 K (green triangles). Solid lines are from theory. As indicated by the data of Fiquet *et al.*'s data experimental errors increase with temperature.

where  $c_{ij}(P', T')$  is the elastic constant tensor given in Eq. (4).  $c_{ij}(P', T')$  for  $\text{MgSiO}_3$  pv has already been determined (Ref. 14). The correction is then carried out by evaluating the strains  $\epsilon_i$  involved in the relaxation of these deviatoric thermal stresses,

$$\epsilon_i(P', T') = \sum_j \kappa_{ij}(P', T') \delta\sigma_j. \quad (8)$$

Figure 5 shows the resulting corrections on the lattice parameters as a function of volume at various  $T$ 's, combined with the experimental temperature dependent data of Fiquet *et al.*<sup>4</sup> and Funamori *et al.*<sup>5</sup> These high temperature data were collected nonsystematically therefore, the trends of deviations with temperature are not systematic either. Besides, uncertainties in pressure scales at high temperatures are also large, which further obscures these trends. It appears clearly that the magnitude of the errors in the lattice parameters increase with  $T$ . This error could be caused by anharmonic effects, but it could also be caused by thermally induced deviatoric stresses. Because the agreement with experiments improves considerably after the relaxation of deviatoric ther-

mal stresses, especially in the range of temperatures of the data of Fiquet *et al.*, up to 2668 K,<sup>4</sup> and of Funamori *et al.*, up to 2000 K,<sup>5</sup> we conclude that these deviations are caused by these stresses. After the relaxation of deviatoric thermal stresses according to Eq. (8), the agreement with experiments improves considerably, especially in the high temperature ranges of the data of Fiquet *et al.*'s, between 1501 and 2668 K,<sup>4</sup> and of Funamori *et al.*, between 400 and 1500 K.<sup>5</sup> Corrections of elastic constants to first order are also possible and should be done, but these will be discussed somewhere else.

#### IV. SELF CONSISTENT QUASIHARMONIC APPROXIMATION

These results indicate that QHA predictions of thermodynamics and structural properties, which are already in excellent agreement with experiments within the domain of validity of this approximation, can be further improved, particularly the crystal structure, if computations include the relaxation of deviatoric thermal stresses. This can be accomplished by an iterative scheme. After thermal stresses are completely relaxed, static energies, phonons, and the free energy,

$$F(V, P', T') = \left\{ U[V(P', T')] + \sum_{\mathbf{q}j} \frac{\hbar \omega_{\mathbf{q}j}[V(P', T')]}{2} \right\} + k_B T' \sum_{\mathbf{q}j} \ln(1 - e^{\hbar \omega_{\mathbf{q}j}[V(P', T')]/k_B T'}), \quad (9)$$

should be recomputed, and so should Eqs. (2)–(4), along with Eqs. (7) and (8), until  $\delta\sigma_i$ 's in Eq. (7) are negligible. The small magnitude of  $\delta\sigma_i$ 's (Fig. 4) suggests that one extra cycle in this iterative procedure may suffice.

This iterative scheme apparently involves an excessive number of calculations. However, this systematic procedure minimizes the number of calculations for structures with a larger number of degrees of freedom, as in the present case. Finally, we have focused here on the relaxation of lattice degrees of freedom only, but internal parameters should be relaxed also. The self-consistent scheme should relax forces that develop at high temperatures. In this proposed iterative scheme, forces are only relaxed along with the lattice degrees of freedom, and this may suffice as well, at least for the purpose of computing structural and thermodynamic properties.

This work was supported by NSF Grants No.EAR-0230319, No. EAR-0635990, and No. ITR-0428774. We especially thank Shuxia Zhang from the Minnesota Supercomputing Institute for her assistance with optimizing the PWSCF code performance on the BladeCenter Linux Cluster.

- <sup>1</sup>D. C. Wallace, *Thermodynamics of Crystals* (Dover, Mineola, 1972).
- <sup>2</sup>P. Hohenberg and W. Kohn, Phys. Rev. **136**, B864 (1964); W. Kohn and L. J. Sham, Phys. Rev. **140**, A1133 (1965).
- <sup>3</sup>Y. Kuwayama, K. Hirose, N. Sata, and Y. Ohishi, Science **309**, 923 (2005).
- <sup>4</sup>G. Fiquet, D. Andrault, A. Dewaele, T. Charpin, M. Kunz, and D. Hausermann, Phys. Earth Planet. Inter. **105**, 21 (1998).
- <sup>5</sup>N. Funamori, T. Yagi, W. Utsumi, T. Kondo, T. Ushida, and M. Funamori, J. Geophys. Res. **101**, 8257 (1996).
- <sup>6</sup>N. Ross and R. Hazen, Phys. Chem. Miner. **16**, 415 (1989).
- <sup>7</sup>N. Ross and R. Hazen, Phys. Chem. Miner. **17**, 228 (1990).
- <sup>8</sup>W. Utsumi, N. Funamori, T. Yagi, E. Ito, T. Kikegawa, and O. Shimomura, Geophys. Res. Lett. **22**, 1005 (1995).
- <sup>9</sup>Y. Wang, D. Weidner, R. Liebermann, and Y. Zhao, Phys. Earth Planet. Inter. **83**, 13 (1994).
- <sup>10</sup>R. M. Wentzcovitch, Phys. Rev. B **44**, 2358 (1991).
- <sup>11</sup>S. Baroni, A. Dal Corso, S. de Gironcoli, P. Giannozzi, C. Cavazzoni, G. Ballabio, S. Scandolo, G. Chiarotti, P. Focher, A. Pasquarello, K. Laasonen, A. Trave, R. Car, N. Marzari, and A. Kokalj, <http://www.pwscf.org/>
- <sup>12</sup>S. Baroni, S. de Gironcoli, A. Dal Corso, and P. Giannozzi, Rev. Mod. Phys. **73**, 515 (2001).
- <sup>13</sup>B. B. Karki, R. M. Wentzcovitch, S. de Gironcoli, and S. Baroni, Phys. Rev. B **62**, 14750 (2000).
- <sup>14</sup>R. M. Wentzcovitch, B. B. Karki, M. Cococcioni, and S. de Gironcoli, Phys. Rev. Lett. **92**, 018501 (2004).
- <sup>15</sup>O. L. Anderson, *Equations of State of Solids for Geophysics and Ceramic Science* (Oxford University Press, New York, 1995).
- <sup>16</sup>A. Zerr and R. Boehler, Science **262**, 553 (1993).
- <sup>17</sup>L. D. Landau and E. M. Lifshitz, *Statistical Physics* (Addison-Wesley, Reading, MA, 1958).
- <sup>18</sup>P. F. Choquard, *The Anharmonic Crystal* (Benjamin, New York, 1967).
- <sup>19</sup>R. Boehler, Rev. Geophys. **38**, 221 (2000).
- <sup>20</sup>T. Tsuchiya, J. Tsuchiya, K. Umemoto, and R. M. Wentzcovitch, Earth Planet. Sci. Lett. **224**, 241 (2004).

**Erratum: First-principles prediction of crystal structures at high temperatures  
using the quasiharmonic approximation  
[Phys. Rev. B 76, 064116 (2007)]**

Pierre Carrier, Renata Wentzcovitch, and Jun Tsuchiya  
(Received 16 October 2007; published 5 November 2007)

DOI: [10.1103/PhysRevB.76.189901](https://doi.org/10.1103/PhysRevB.76.189901) PACS number(s): 62.20.Dc, 65.40.-b, 91.35.-x, 91.60.Gf, 99.10.Cd

Equation (6) had a sign mistyped. It should read

$$\alpha = \frac{1}{V} \left. \frac{\partial V}{\partial T} \right|_{P'}.$$

Equation (9) is the thermodynamic functional relation for  $F$  that depends on the two independent variables:  $V(P', T')$  and  $T'$ . Therefore, Eq. (9) should read

$$F[V(P', T'), T'] = \left\{ U[V(P', T')] + \sum_{\mathbf{q}j} \frac{\hbar \omega_{\mathbf{q}j}[V(P', T')]}{2} \right\} + k_B T' \sum_{\mathbf{q}j} \ln(1 - e^{\hbar \omega_{\mathbf{q}j}[V(P', T')]/k_B T'}).$$